www.nature.com/cdd

CDDpress

ARTICLE

MAP2K6 remodels chromatin and facilitates reprogramming by activating Gatad2b-phosphorylation dependent heterochromatin loosening

Guangsuo Xing[1,2,5], Zichao Liu[1,2,3,5], Luyuan Huang[1,2,3,5], Danyun Zhao[1,2,3,5], Tao Wang[1,2], Hao Yuan[1,2], Yi Wu[1,2], Linpeng Li[1,2], Qi Long[1,2], Yanshuang Zhou[1,2], Zhihong Hao[1,2,3], Yang Liu[1,2,3], Jianghuan Lu[1,2], Shiting Li[1,2], Jieying Zhu[1,2], Bo Wang[1,2], Junwei Wang[1,2], Jing Liu[1,2], Jiekai Chen[1,2], Duanqing Pei[1,2,4✉], Xingguo Liu[1,2,4✉] and Keshi Chen[1,2✉]

Somatic cell reprogramming is an ideal model for studying epigenetic regulation as it undergoes dramatic chromatin remodeling. However, a role for phosphorylation signaling in chromatin protein modifications for reprogramming remains unclear. Here, we identified mitogen-activated protein kinase kinase 6 (Mkk6) as a chromatin relaxer and found that it could significantly enhance reprogramming. The function of Mkk6 in heterochromatin loosening and reprogramming requires its kinase activity but does not depend on its best-known target, P38. We identified Gatad2b as a novel target of Mkk6 phosphorylation that acts downstream to elevate histone acetylation levels and loosen heterochromatin. As a result, Mkk6 over-expression facilitates binding of Sox2 and Klf4 to their targets and promotes pluripotency gene expression during reprogramming. Our studies not only reveal an Mkk phosphorylation mediated modulation of chromatin status in reprogramming, but also provide new rationales to further investigate and improve the cell fate determination processes.

Cell Death & Differentiation (2022) 29:1042–1054; https://doi.org/10.1038/s41418-021-00902-z

INTRODUCTION

Induced pluripotent stem cells (iPSCs) can be obtained by introducing three or four transcriptional factors into mouse embryonic fibroblasts, and the somatic cell reprogramming process is accompanied by dramatic changes in epigenetics and chromatin structure [1]. Histone acetylation and methylation in reprogramming have been extensively studied. The acetylation levels of histones are elevated during reprogramming and many histone deacetylase inhibitors, such as VPA and sodium butyrate are used to promote reprogramming [2–4]. Changes of histone methylation during reprogramming are more complex. The methylation levels of H3K4 are increased in the promoter regions of most active genes while the methylation levels of H3K27 are decreased at the same sites [4]. Wdr5, an effector of H3K4 methylation, was reported to enhance reprogramming [5], while H3K27 demethylases Utx and Jmjd3 have divergent effects, improving and blocking reprogramming, respectively [6, 7]. H3K36 demethylases Jhdm1a/1b not only enhance reprogramming, but also enable efficient generation of iPSCs by Oct4 alone [8, 9]. Finally, high levels of H3K9 methylation block reprogramming and demethylation of H3K9 can convert pre-iPSCs to fully reprogrammed iPSCs [10].

Chromatin remodeling complexes also play important roles in reprogramming [11]. Components of swith/sucrose nonfermentable (SWI/SNF) complex, Brg1 and BAF155, are directly recruited by Oct4 to relax chromatin structure and enhance reprogramming [12]. Similarly, the chromodomain helicase DNA-binding (CHD) remodeling factor Chd1 and subunit of inositol-requiring (INO) complex Ino80 both were reported to maintain open chromatin that strongly increases the reprogramming efficiency [13, 14]. In contrast, components of the repressive MeCP1-Mi-2/nucleosome remodeling and deacetylase (NuRD) complex including HDAC1 and Mbd2/3, impair iPSC formation [15]. The studies of Mbd3 in reprogramming are conflicting. It's reported that Mbd3 is a deterministic factor in reprogramming, as 100% of the cells depletion of Mbd3 become iPSCs [16]. Another study agreed with the enhancement of Mbd3 silencing in reprogramming, but not to a deterministic level [15]. However, it has recently been shown that Mbd3 is required in reprogramming to naïve pluripotent state [17].

Previously, we showed significant heterochromatin relaxation mediated by Oct4 at the initial stage of reprogramming and identified Gadd45a as a chromatin relaxer which also enhances iPSCs induction [18]. Beside of Gadd45a, we have screened out Mkk6, a kinase belongs to the mitogen-activated protein kinases

[1]CAS Key Laboratory of Regenerative Biology, Joint School of Life Sciences, Guangzhou Institutes of Biomedicine and Health, Chinese Academy of Sciences; Bioland Laboratory (Guangzhou Regenerative Medicine and Health Guangdong Laboratory), Guangzhou Medical University, 510530 Guangzhou, China. [2]Guangdong Provincial Key Laboratory of Stem Cell and Regenerative Medicine, CUHK-GIBH Joint Research Laboratory on Stem Cells and Regenerative Medicine, Institute for Stem Cell and Regeneration, Guangzhou Institutes of Biomedicine and Health, Chinese Academy of Sciences, 510530 Guangzhou, China. [3]University of Chinese Academy of Sciences, Beijing, China. [4]Centre for Regenerative Medicine and Health, Hong Kong Institute of Science & Innovation, Chinese Academy of Sciences, Hong Kong SAR, China. [5]These authors contributed equally: Guangsuo Xing, Zichao Liu, Luyuan Huang, Danyun Zhao. ✉email: peiduanqing@westlake.edu.cn; liu_xingguo@gibh.ac.cn; chen_keshi@gibh.ac.cn

Edited by D Aberdam

Received: 23 April 2021 Revised: 3 November 2021 Accepted: 10 November 2021
Published online: 24 November 2021

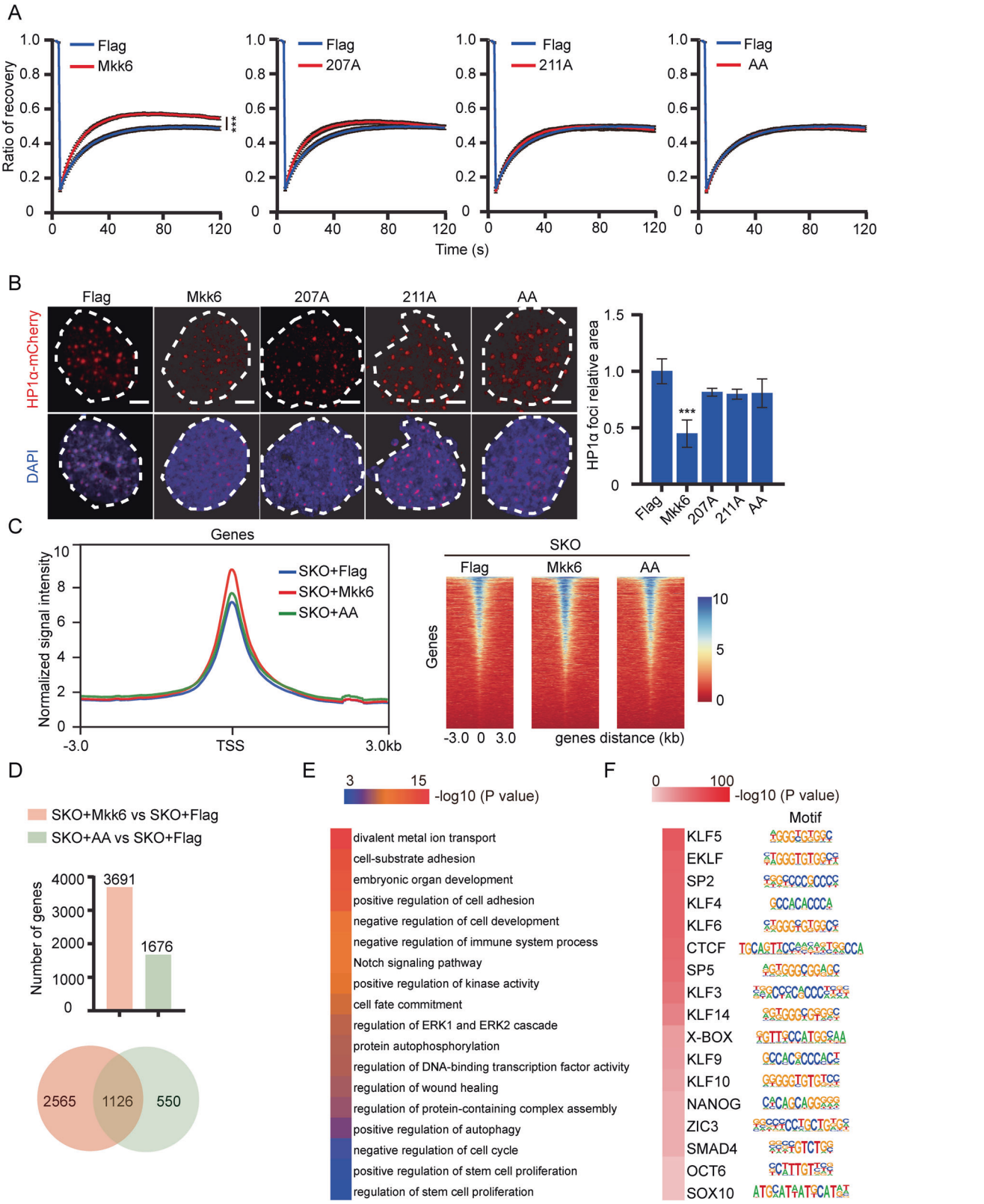

(MAPK) pathways, which not only relaxes heterochromatin, but also improves the 7 F (Jdp1, Jhdm1b, Mkk6, Glis1, Nanog, Esrrb and Sall4) reprogramming [19]. However, the mechanism by which Mkk6 regulates heterochromatin relaxation and pluripotency acquisition is still unclear. In this work, we validate Mkk6 as a heterochromatin relaxer and show that it can significantly improve Sox2, Klf4, Oct4 (SKO) and Sox2, Klf4, Oct4, c-Myc (SKOM) induced reprogramming, dependent on its kinase activity but not via its classical downstream target, P38. We identified Gatad2b, a subunit of the NuRD complex, as a novel target of Mkk6. Phosphorylation of Gatad2b by Mkk6

Fig. 1 Mkk6 is a heterochromatin relaxer. A Fluorescence recovery kinetics of heterochromatin in MEFs infected with Flag, Mkk6 and its mutants. More than 20 cells were analyzed for each group. Data were shown as mean ± SEM. ***$p \leq 0.001$. **B** Immunofluorescence detection of HP1α foci in MEFs transfected with Mkk6 or its mutants. Mkk6, but not 207 A, 211 A or AA mutants, significantly decreased the relative HP1α amount. More than 72 cells were analyzed for each group. Data were shown as mean ± SD. ***$p \leq 0.001$. Scale bar: 5 μm. **C** Metagene plot of ATAC-seq signal in MEFs infected with SKO + Flag, SKO + Mkk6 and SKO + AA. **D** Number of genes with more accessible chromatin in MEFs infected with SKO + Mkk6 and SKO + AA, compared with SKO + Flag control. Venn diagram depicting overlap between them was shown. **E** Gene Ontology (GO) analysis for the genes with more accessible chromatin in MEFs infected with SKO + Mkk6 compared with SKO + AA. **F** Transcription factor motif analysis of genes with more accessible chromatin in MEFs infected with SKO + Mkk6, compared with SKO + AA. The motifs for transcription factors are indicated on the right of the heatmap.

leads to elevated histone acetylation levels and heterochromatin loosening. Our studies reveal the relationship between Mkk6 kinase activity, chromatin status and reprogramming, shedding light on the control of cell fate determination by phosphorylation signaling.

RESULTS

Mkk6 is a heterochromatin relaxer

Mitogen-activated protein kinase signaling pathways have been shown to play important roles in cell fate transition [20–22]. As we previously demonstrated that Mkk6 is required in the 7F induced reprogramming through chromatin remodeling [19], we hypothesized that Mkk6 might be a heterochromatin relaxer and also important in SKO and SKOM induced reprogramming. We first employed a fluorescence recovery after photobleaching (FRAP) method to assess the effects of Mkk6 on heterochromatin dynamics [18, 23]. We labeled HP1α with mCherry to distinguish heterochromatin and euchromatin and histone H1 with GFP to perform FRAP assay (Supplementary Fig. S1A). By selecting region of interest within HP1α foci, we found Mkk6 increased the heterochromatin dynamics significantly as assayed by FRAP (Fig. 1A and Supplementary Fig. S1B). We then quantified heterochromatin with HP1α stain and observed a decrease in HP1α foci in MEFs infected with Mkk6 (Fig. 1B). To verify and extend the FRAP experiments to endogenous proteins, we tested the association of structural proteins with chromatin (histones) by biochemical extraction [24]. Upon salt extraction of isolated nuclei, fractions of H3 were released at lower salt concentrations in MEFs infected with Mkk6 than controls (Supplementary Fig. S1C). These results suggest Mkk6 is a heterochromatin relaxer.

To test whether Mkk6 relaxes heterochromatin through its kinase activity, we mutated its activating phosphorylation sites to generate dominant negative, phospho-deficient mutants of Mkk6 (207 A, 211 A, double mutant AA) (Supplementary Fig. S1D) [25]. Mkk6 dominant negative mutants showed no increase in dynamic heterochromatin indicated by FRAP and HP1α staining, indicating Mkk6 opens heterochromatin through its kinase activity (Fig. 1A–D and Supplementary Fig. S1B).

To understand the details of heterochromatin relaxation by Mkk6 in reprogramming, we performed transposase-accessible chromatin sequencing (ATAC-seq) on MEFs infected with Flag control, Mkk6 and double mutant AA (AA) undergoing SKO induced reprogramming. Quantification of the ATAC-seq signal showed that the normalized signal intensity in Mkk6 was much higher than in Flag and AA, indicating heterochromatin underwent significant relaxation in the presence of Mkk6 during reprogramming (Fig. 1C). There were 3691 gene loci with more accessible chromatin identified in Mkk6 compared with Flag in reprogramming, and most gene loci opened in Mkk6 were closed in AA mutant (2565 out of 3691) (Fig. 1D). Gene Ontology (GO) analysis of these genes showed that genes opened by Mkk6 in reprogramming were associated with ion transport, cell adhesion, cell development, etc (Fig. 1E). We next analyzed the transcription factor motifs associated with the genes and found they were enriched for pluripotency-related motifs such as Klf, Nanog and Sox (Fig. 1F).

Mkk6 enhances somatic cell reprogramming

We then asked whether Mkk6 enhances SKO and SKOM induced reprogramming and found that Mkk6 over-expression not only improved but also accelerated the SKO or SKOM induced reprogramming kinetics, such that the first GFP + colony appears earlier than control (Fig. 2A). The resulting iPSC clones have been characterized for several pluripotency markers, and shown to give rise to chimeric mice capable of undergoing germline transmission (Supplementary Fig. S2A–C). Furthermore, Mkk6 over-expression can prevents the formation of partially reprogrammed cells, so called pre-iPSCs in SKOM induced reprogramming (Fig. 2B), and Mkk6 could also promote the transition from pre-iPSCs to iPSCs (Fig. 2C). In addition, Mkk6 can rescue Oct4-L80A mutant, which is incapable of inducing reprogramming [26], to generate iPSCs efficiently, confirming its role in relaxing heterochromatin (Fig. 2D).

There are seven members in the Mkk family, and we overexpressed each of them during both SKO and SKOM induced reprogramming. Over-expression of either Mkk3 or Mkk6 significantly increased the reprogramming efficiency (Fig. 2E). Mkk3 and Mkk6 have similar structures and functions [27, 28]. There is no additive effect on reprogramming when over-expressing Mkk3 and Mkk6 together, indicating that they likely function through the same downstream target (Fig. 2F and Supplementary Fig. S2D). To further analyze the role of Mkk3 and Mkk6 in reprogramming, we also knocked them down using shRNA vectors (Supplementary Fig. S2E). The reprogramming efficiency was reduced by the shRNAs, indicating Mkk3 and Mkk6 are required for effective reprogramming (Fig. 2G and Supplementary Fig. S2F). Moreover, Mkk3 could also promote the transition from pre-iPSCs to iPSCs (Supplementary Fig. S2G).

We then used the dominant negative, phospho-deficient mutants of Mkk6 (207 A, 211 A, double mutant AA) and its constitutively active, phospho-mimetic mutants (207E, 211E, double mutant EE) to test whether Mkk6 enhances reprogramming through its kinase activity [25]. Over-expression of the three dominant negative mutants of Mkk6 had no effects on either SKO or SKOM induced reprogramming while the three dominant active mutants had similar augmenting effects as wild-type Mkk6 (Fig. 2H and Supplementary Fig. 2H). Further, Mkk6 dominant negative mutants couldn't promote the transition from pre-iPSCs to iPSCs or rescue Oct4 L80A deficiency in reprogramming (Fig. 2C, D). These results indicate that Mkk6 enhances reprogramming depending on its kinase activity.

Mkk6 enhances reprograming through phosphorylation of Gatad2b, not P38

P38 MAPKs are well-characterized targets of Mkk6 [29], however the role of P38 in reprogramming is controversial [30, 31]. We found that during reprogramming the total protein level of P38 was not affected by expression of wild-type (WT) Mkk6 or its mutants, while the level of phosphorylated P38 was elevated by WT Mkk6, but not 207 A and AA Mkk6 (Supplementary Fig. S3A–C). These results indicate that P38 is activated by over-expressing WT Mkk6 in reprogramming. However, over-expression of each of the four P38 MAPKs was unable to improve the reprogramming as Mkk6 did, while silencing P38 by shRNA couldn't inhibit reprogramming with

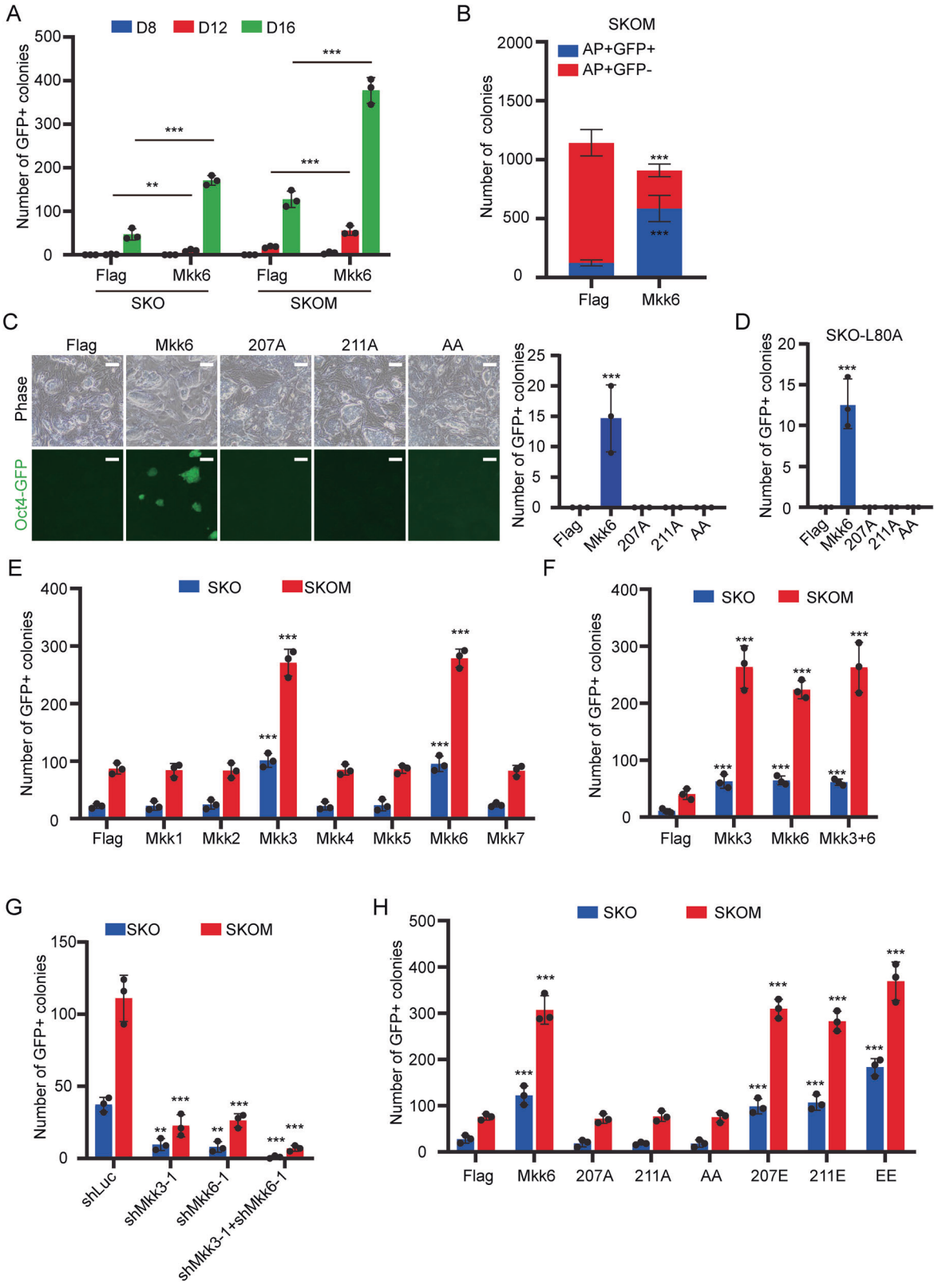

or without Mkk6 (Supplementary Fig. S3D–F). Together, these results indicate that Mkk6-mediated activation of P38 is not important for efficient reprogramming. Exploring the new targets of Mkk6 is necessary for better understanding its roles in cell fate transition.

To identify the potential target proteins of Mkk6 in reprogramming, we performed phospho-ITRAQ experiments (Supplementary Fig. S3G) [32–34]. We identified several proteins that were upregulated in Mkk6 reprogramming but not in 207 A

Fig. 2 Mkk6 enhances reprogramming. A Mkk6 greatly accelerates the kinetics of SKOM or SKO induced reprogramming. Data were from three independent experiments and were shown as mean ± SD. $^{**}p \le 0.01$; $^{***}p \le 0.001$. **B** Mkk6 over-expression prevents the formation of partially reprogrammed cells. OG2 MEFs were reprogrammed by SKOM + Flag or SKOM + Mkk6 in mES medium. The iPS colonies were stained with alkaline phosphatase (AP); the numbers of AP + GFP + colonies and AP + GFP- colonies were counted. Data were from three independent experiments and were shown as mean ± SD. $^{***}p \le 0.001$. **C** Mkk6 over-expression converts pre-iPSCs into iPSCs. Data were from three independent experiments and were shown as mean ± SD. $^{***}p \le 0.001$. Scale bar, 100 μm. **D** Reprogramming efficiency with SKO-L80A plus Mkk6 or its mutants. Data were from three independent experiments and were shown as mean ± SD. $^{***}p \le 0.001$. **E** Effects of over-expression of Mkk family members on SKO or SKOM induced MEF reprogramming; the numbers of GFP + colonies were counted. Data were from three independent experiments and were shown as mean ± SD. $^{***}p \le 0.001$. **F** Mkk3 and Mkk6 were overexpressed individually and together in a separate reprogramming experiment. Data were from three independent experiments and were shown as mean ± SD. $^{***}p \le 0.001$. **G** Reprogramming efficiency was inhibited by shRNA silencing of Mkk3 or Mkk6. Data were from three independent experiments and were shown as mean ± SD. $^{**}p \le 0.01$; $^{***}p \le 0.001$. **H** Effects of over-expression of Mkk6 dominant negative (207 A, 211 A, double mutation AA) and constitutively active (207E, 211E, double mutation EE) mutants on SKO and SKOM induced reprogramming; the number of GFP + colonies were counted. Data were from three independent experiments and were shown as mean ± SD. $^{***}p \le 0.001$.

or AA mutant (Supplementary Fig. S3H, Supplementary Table S1 and S2). By analyzing the biological process annotations of these proteins, we found Gatad2b, a member of the NuRD complex that is involved in histone acetylation (Fig. 3A, B). Co-Immunoprecipitation showed that Mkk6 interacted with Gatad2b (Fig. 3A). Then we tested whether phospho-Gatad2b is related to Mkk6 in reprogramming. We purified Gatad2b proteins by immunoprecipitation (IP) using anti-Gatad2b in SKO + Flag, SKO + Mkk6, SKO + 207 A and SKO + AA cell lysate, and then detected phospho-Gatad2b in the resulting fractions using anti-p-Ser/Thr while the total Gatad2b was used as reference. These experiments showed that phospho-Gatad2b was upregulated in reprogramming with Mkk6, but not with 207 A or AA mutant (Fig. 3B). Further, we showed Mkk3 but not its dominant negative mutants (218 A and 3AA) could increase the phosphorylation of Gatad2b (Fig. 3C).

To verify whether Mkk6 relaxes heterochromatin through Gatad2b, we designed shRNAs of Gatad2b to knock down its expression in reprogramming and performed ATAC-seq (Fig. 3D and supplementary Fig. S3E). The normalized signal intensity in SKO with Gatad2b silencing is much lower than that of SKO with and without Mkk6 (Fig. 3D). Most of the gene loci that opened by Mkk6 were closed by Gatad2b silencing in reprogramming (3567 out of 3691) (Fig. 3E). Similar to AA mutant, GO analysis showed that genes closed by Gatad2b in reprogramming were associated with cell development, ion transport, cell adhesion, etc (Fig. 3F), and the transcription factor motifs analysis showed the genes were enriched for Klf, Nanog and Sox, too (Fig. 3G).

Next, we found Gatad2b over-expression did not have effects on reprogramming under normal conditions (Fig. 3H). However, Gatad2b silencing by shRNAs not only decreased the efficiency of SKO induced reprograming, but also impaired the increase of reprograming efficiency by Mkk6 over-expression (Fig. 3I and Supplementary Fig. S3I). Similarly, Gatad2b silencing blocked the increase of reprograming efficiency by Mkk3 over-expression (Supplementary Fig. S3J). These results suggested that Mkk6 relaxes heterochromatin and enhances reprogramming through phosphorylation of Gatad2b.

Mkk6 phosphorylates Gatad2b at S487 and T490

To explore the details of Mkk3/6-dependent Gatad2b phosphorylation, we conducted an in vitro kinase assay using IP-purified Mkk6-HA, AA-HA, Mkk3-HA and Gatad2b-3Flag (Supplementary Fig. S4A). The results showed that Mkk3 and Mkk6, but not AA directly phosphorylated Gatad2b (Fig. 4A). Given that Mkk3/6 phosphorylates Gatad2b, we mapped the phosphorylation sites within Gatad2b by mass spectrometry after the in vitro kinase assay. We observed the phosphorylation at Ser487 and Thr490 was specifically promoted by Mkk3/6 (Fig. 4B and Supplementary Fig. S4B). To further verify these identified phosphorylation sites, we mutated the S487 and T490 to alanine (STAA) to generate dominant negative, phospho-deficient mutants of Gatad2b. We overexpressed Gatad2b and STAA in reprogramming with and without Mkk3/6 and showed that Mkk3/6 could phosphorylate Gatad2b but not STAA (Fig. 4C and Supplementary Fig. S4C). We also performed in vitro kinase assay by using IP-purified Mkk6-HA, Mkk3-HA and Gatad2b-3Flag, STAA-3Flag, and confirmed that Mkk3/6 phosphorylates Gatad2b at S487 and T490 (Fig. 4D and Supplementary Fig. S4D).

Mkk6 elevates histone acetylation levels through Gatad2b

Gatad2b is a member of the NuRD complex that is involved in histone acetylation, and we tested whether Gatad2b directly interacts with histone acetylation sites. Co-Immunoprecipitation showed that H3k9ac, H3K27ac and H4K16ac interacted with Gatad2b (Supplementary Fig. S5A). We also showed that in the presence of VPA, a broad-spectrum HDAC inhibitor, there was no additive effect of Mkk6 on reprogramming, implicating Mkk6 in the regulation of histone acetylation (Supplementary Fig. S5B).

To test this hypothesis, we analyzed the acetylation of histones by western blot. We found WT Mkk6 but not its dominant negative mutants increased the acetylation levels of H3K9, H3K27 and H4K16 (Fig. 5A). These histone acetylation levels were all decreased when endogenous Gatad2b was knocked down by shRNA (Fig. 5B). Gatad2b silencing also blocked the increase of histone acetylation by Mkk6 over-expression (Fig. 5B). To further investigate the Mkk6-induced histone modifications, we performed H3K9ac ChIP-seq in reprogramming on day 8 (Fig. 5C). We found that the H3K9ac signal around the TSSs increased markedly in the presence of Mkk6, but not AA (Fig. 5C). When endogenous Gatad2b was knocked down, the H3K9ac signal around the TSSs significantly decreased (Fig. 5C). Gatad2b silencing also blocked the increase of the H3K9ac signal around the TSSs by Mkk6 over-expression (Fig. 5C), consistent with western blot results. We then measured the level of H3K9ac around all TSSs and collected all those showing 1.5-fold upregulated (Fig. 5D, E). Most of the genes hyperacetylated by Mkk6 were deacetylated by AA mutant (5454 out of 6767) or Gatad2b silencing (4980 out of 6767) (Fig. 5D, E). GO analysis showed these genes were associated with cell cycle, chromosome organization, histone modification, etc (Supplementary Fig. S5C, D). In addition, we confirmed that Mkk6 increased the H3K9ac, H3K27ac and H4K16ac levels in the promoter regions of pluripotency genes such as *Oct4*, *Sox2* and *Nanog* by ChIP-qPCR (Fig. 5F). The acetylation levels of H3K9, H3K27 and H4K16 in these promoter regions were all decreased by shGatad2b alone or in the presence of Mkk6 (Fig. 5G). Altogether, these data demonstrate that Mkk6 increases histone acetylation by phosphorylating and consequently activating Gatad2b.

Mkk6 facilitates the binding ability of Sox2 and Klf4 and promotes the expression of pluripotency genes

To establish a causal relationship between the Mkk6-induced open chromatin structure and reprogramming, we analyzed the

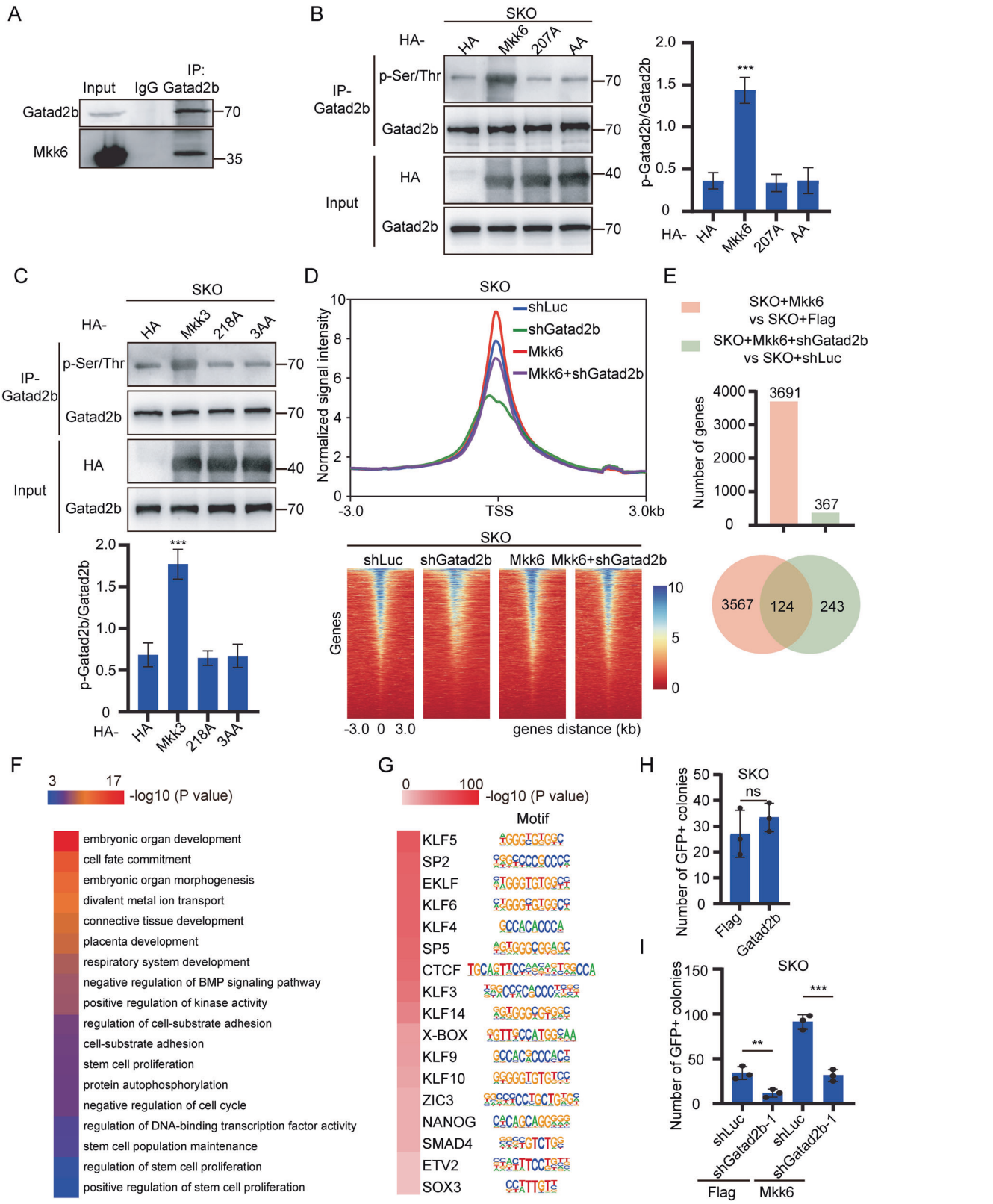

chromatin status of pluripotency genes such as *Oct4*, *Nanog*, *Sox2*, etc. We found the promoter regions of these genes are more accessible and hyperacetylated in SKO reprogramming with Mkk6 overexpression (Supplementary Fig. S6A). A nuclease accessibility assay was used to confirm the chromatin status of pluripotency gene [18, 35]. We showed that MEFs infected with Mkk6 displayed open structure that are susceptible to nuclease digestion in the promoter region of *Oct4* (Fig. 6A). Considering the transcription

Fig. 3 Mkk6 relaxes heterochromatin and enhances reprogramming through phosphorylation of Gatad2b. A Co-immunoprecipitation of Mkk6 and Gatad2b indicated interaction between them. **B** The levels of total and phosphorylated Gatad2b (p-Gatad2b) were detected by western blot in MEFs infected with SKO plus Flag, Mkk6 or its mutants. Quantitative analysis of phosphorylated Gatad2b to total Gatad2b was shown. Data were from three independent experiments and were shown as mean ± SD. ***$p \le 0.001$. **C** The levels of total and phosphorylated Gatad2b (p-Gatad2b) were detected by western blot in MEFs infected with SKO plus Flag, Mkk3 or its mutants. Quantitative analysis of phosphorylated Gatad2b to total Gatad2b was shown. Data were from three independent experiments and were shown as mean ± SD. ***$p \le 0.01$. **D** Metagene plot of ATAC-seq signal in MEFs infected with SKO + shLuc, SKO + shGatad2b, SKO + Mkk6 and SKO + Mkk6 + shGatad2b. **E** Number of genes with more accessible chromatin in MEFs infected with SKO + Mkk6 and SKO + Mkk6 + shGatad2b, compared with SKO + Flag or SKO + shLuc control separately. Venn diagram depicting overlap between them was shown. **F** GO analysis for the genes with more accessible chromatin in MEFs infected with SKO + Mkk6, compared with SKO + Mkk6 + shGatad2b. **G** Transcription factor motif analysis of genes with more accessible chromatin in MEFs infected with SKO + Mkk6, compared with SKO + Mkk6 + shGatad2b. The motifs for transcription factors are indicated on the right of the heatmap. **H** Effects of overexpression of Gatad2b on SKO induced reprogramming; the number of GFP + colonies were counted. Data were from three independent experiments and were shown as mean ± SD. **I** Effects of shGatad2b on reprogramming in the presence or absence of Mkk6; the number of GFP + colonies were counted. Data were from three independent experiments and were shown as mean ± SD. **$p \le 0.01$; ***$p \le 0.001$.

factor motifs such as Klf, Sox and Oct were opened by Mkk6 in reprogramming, we then carried on ChIP-qPCR to assess the binding of the three Yamanaka factors (Oct4, Sox2 and Klf4) to their targets in reprogramming (Figs. 1F and 3G). We showed that, on day 8 Sox2 and Klf4 bound to their targets more readily when co-expressed with WT Mkk6, but not the 207 A or AA mutants (Fig. 6B). The binding properties of Oct4 were not affected by Mkk6 (Supplementary Fig. S6B). As a result, RNA-seq analysis showed that the expression of the pluripotency genes, such as *Cdh1*, *Nanog*, *Oct4*, *Sox2*, etc was enhanced by Mkk6 but not AA (Fig. 6C). RT-qPCR analysis confirmed that the expression levels of pluripotency genes such as endogenous *Oct4*, *Nanog, Rex1* and *Sox2* increased significantly after Mkk6 induction during reprogramming (Fig. 6D).

DISCUSSION

MAPK pathways receive a variety of extracellular stimuli and play critical roles in many biological responses such as cell growth and apoptosis [22, 36]. The central core of each MAPK pathway is a conserved cascade of three kinases: MAPK, Mkk and MTK [37]. Though MAPK proteins such as Erk1/2, Jnk1/2/3, P38 are well studied, there is few reports about the function of Mkk proteins. Here we revealed a new function of Mkk6 as a chromatin relaxer that can open heterochromatin dependent on its kinase activity (Fig. 6E). Since histones and many epigenetic enzymes can be phosphorylated [38–40], we sought to explore the relationship between Mkk6 and histone modification and found that Mkk6 interacts with and phosphorylates Gatad2b, leading to increased H3K9, H3K27 and H4K16 acetylation levels during reprogramming, in turn, leading to upregulated expression of pluripotency genes (Fig. 6E). Our work indicates that Mkk6 may regulate gene expression through histone modification and elucidates a new signaling pathway between extracellular stimuli and intracellular gene expression.

P38 MAPK is the classic target of Mkk6 in MAPK signaling pathway and was reported to enhance mouse somatic cell reprogramming [31], but the role of P38 MAPK in reprogramming remains controversial [30]. Recently, we found that Mkk6 was involved in the 7 F induced reprogramming [19], but the mechanism remains unclear. In the present work, we tested the effects of Mkks on reprogramming and found that Mkk3 and Mkk6 can improve reprogramming in a manner that depends on their kinase activities, but not on P38. These results implied that Mkk6 have other targets awaiting identification. Mkk6 are not only P38 activators, but also of importance in other pathways. It was reported that Mkk6 could interact with and phosphorylate p66shc in β-Amyloid-mediated cell toxicity [41]. In our study, we identified Gatad2b, a novel target of Mkk6, by phospho-ITRAQ. Gatad2b, also called p66b, belongs to NuRD complex [42]. Gatad2b recruits Mbd2, another component of NuRD complex, to DNA and histones and affects the deacetylation of histones and repression of transcription [43, 44]. Gatad2b was recently reported to be sumoylated to enhance the formation of NuRD complex [45], whereas, in our work, we found an opposing regulation of Gatad2b by Mkk6 phosphorylation that elevates histone acetylation levels and enhances pluripotency gene expression. The underlying molecular mechanisms need further investigation.

NuRD complex is composed of six core subunits with Hdac1/2, Mta1/2/3, RbAP46/48, Chd3/4 and Gatad2a/2b [17, 46]. The roles of these subunits in reprogramming have been studied, but remain controversial. Some reports suggested that Mbd3 inhibits reprogramming [15, 16, 46, 47]. Hanna and colleagues argued that Mbd3 deletion leads to rapid deterministic reprogramming with 100% efficiency and identified Gatad2a-Chd4-Mbd3 as a functional axis underlying inhibition of naïve pluripotency [16, 46]. However, others showed that Mbd3/NuRD enhances reprogramming in a context-dependent manner [17, 48, 49]. Mbd3 was reported to be required in reprogramming from neural stem cells, epiblast stem cells and primary human fibroblasts, but not in reprogramming of MEFs [17, 49]. Another report showed that Sox2 recruited the NuRD complex to mTOR promoter and repressed its transcription, leading to initiation of autophagy which is required for reprogramming [48]. In this study, we showed the phosphorylation of Gatad2b facilitates reprogramming of MEFs. Further examination of these practical differences among different studies may help to define the exact role of NuRD in reprogramming.

There are several reports regarding a role for phosphorylation in reprogramming. A screen of kinase inhibitors identified three kinases that inhibited reprogramming: P38, inositol trisphosphate 3-kinase and Aurora A kinase [30]. Another kinome-wide functional analysis identified some kinases as barriers to iPSC generation and highlighted the role of cytoskeletal remodeling in somatic cell reprogramming [50]. Other reports have found that AMP-activated protein kinase, JNK1/2, Jak/Stat3 and IKK are involved in reprogramming [51–54], however the role of phosphorylation of chromatin proteins in reprogramming has not previously been described. To our knowledge, this is the first indication that Mkk6 plays a role in epigenetic regulation and reprogramming. The activities of many kinases can be regulated by small compounds, potentially providing a new and simple way to further investigation into cell fate transition.

MATERIALS AND METHODS

DNA constructs, cell lines, and cell culture

All constructs for in vitro expression were cloned to pMXs plasmids, and shRNAs were cloned to pSuper plasmids [18]. Point mutation constructs were generated with pMXs-Mkk6 as the template. Primers for 207 A were forward (5′- GGAATCAGTGGCTACCTGGTCGACGCTGTTGCTAAAACGATCGATGCCGGTTGC-3′) and reverse (5′- GCAACCGGCATCGATCGTTTTAGCAACAGCGTCGACCAGGTAGCCACTGATTCC-3′). Primers for 211 A were: forward (5′- GGCTACCTGGTCGACTCTGTTGCTAAAGCGATCGATGCCGGTTGCAAACCATACATGG-3′) and reverse (5′- CCATGTATGGTTTGCAACCGGCATCGATCGCTTTAGCAACAGA

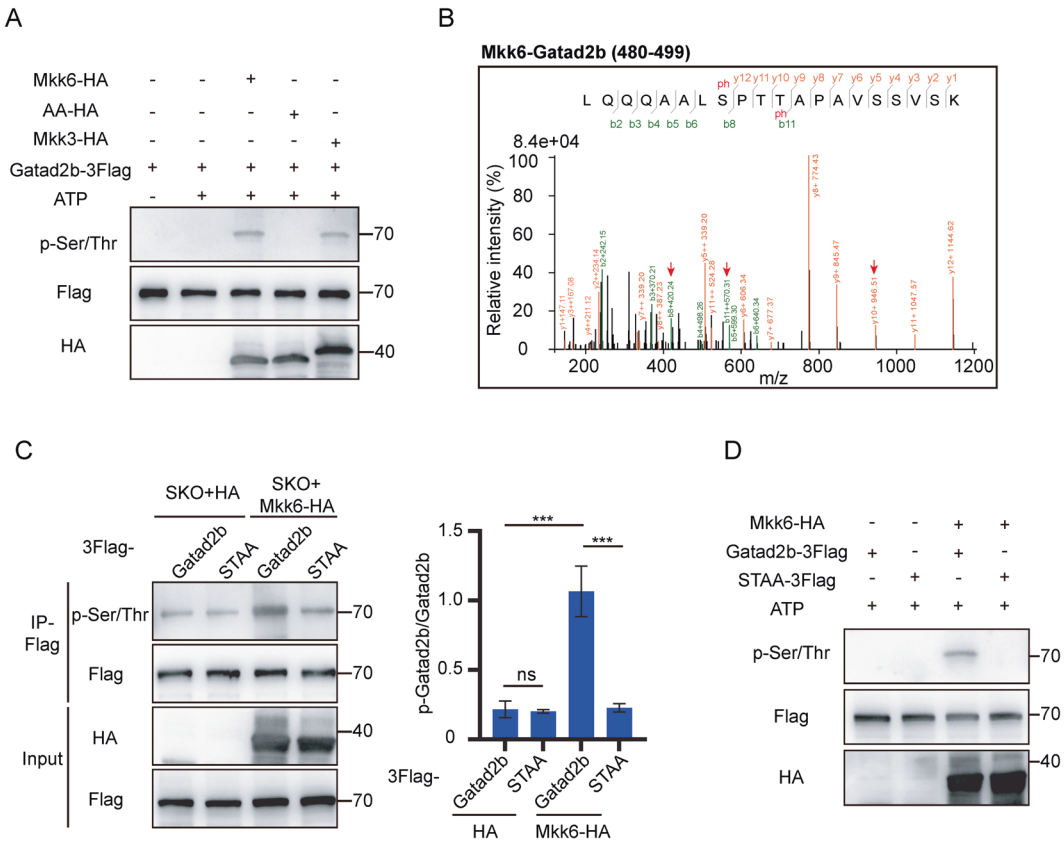

Fig. 4 Mkk6 phosphorylates Gatad2b at S487 and T490. A In vitro kinase assay showing that Mkk6 and Mkk3 phosphorylate Gatad2b. **B** Mass spectrometric analysis of Gatad2b phosphorylation at S487 and T490. **C** S487 and T490 mutation of Gatad2b (STAA) abolishes its phosphorylation by Mkk6. Quantitative analysis of phosphorylated Gatad2b to total Gatad2b was shown. Data were from three independent experiments and were shown as mean ± SD. ***$p \leq 0.001$. **D** In vitro kinase assay showing that Mkk6 phosphorylates Gatad2b, but not STAA.

GTCGACCAGGTAGCC-3′); Primers for AA were: forward (5′- CAGTGGCTA CCTGGTCGACGCTGTTGCTAAAGCGATCGATGCCGGTTGCAAACCATAC-3′) and reverse (5′- GTATGGTTTGCAACCGGCATCGATCGCTTTAGCAACAGCGTCGACCA GGTAGCCACTG-3′). Primers for 207E were forward (5′- GGAATCAGTGGCTAC CTGGTCGACGAAGTTGCTAAAACGATCGATGCCGGTTGC-3′) and reverse (5′- G CAACCGGCATCGATCGTTTTAGCAACTTCGTCGACCAGGTAGCCACTGATTCC-3′). Primers for 211E were: forward (5′- GGCTACCTGGTCGACTCTGTTGCTAAA GAGATCGATGCCGGTTGCAAACCATACATGG-3′) and reverse (5′- CCATGTATG GTTTGCAACCGGCATCGATCTCTTTAGCAACAGAGTCGACCAGGTAGCC-3′); Primers for EE were: forward (5′- CAGTGGCTACCTGGTCGACGAAGTTGCTAAAGA GATCGATGCCGGTTGCAAACCATAC-3′) and reverse (5′- GTATGGTTTGCAACCG GCATCGATCTCTTTAGCAACTTCGTCGACCAGGTAGCCACTG-3′). Primers for STAA Gatad2b were: forward (5′- ACTCGCCCCAACGGCAGCTCCAGCTGTATC-CAGTGTCAGT-3′) and reverse (5′- GAGCTGCCGTTGGGGCGAGTGCTGCCTG CTGCTGTAATCG-3′). The shMkk3 target sequences were 5′-GCATGTGAA-GATGTGCGACTT-3′ and 5′-CCCATTCTTCACCTTGCACAA-3′. The shMkk6 target sequences were 5′-GCCACAGTTAATAGCCAGGAA-3′ and 5′-GCCCACATATC-CAGAGCTTAT-3′. The shP38 target sequences were 5′-CCTCTTGTTGAAA-GATTCCTT-3′ and 5′-CCAACAATTCTGCTCTGGTTA-3′. The shGatad2b target sequences were 5′-CGGATGGAAGAGAGACTCAAA-3′ and 5′-ACAGGAAATT-GAACAGCGATT-3′.

MEFs carrying the Oct4-GFP transgene (OG2-MEFs) were used for reprogramming as described [55]. MEFs and plat-E cells were cultured in DMEM/High Glucose (HyClone) supplemented with 10% fetal bovine serum (FBS) (Gibco). Mouse ESCs and iPSCs were maintained in KSR medium (DMEM/Knock out (Gibco) + 15% KSR (Gibco) + NEAA (Gibco) + GlutaMax (Gibco) + Sodium Pyruvate (Gibco) + β-Mercaptoethanol (Invitrogen) + lif) with feeder cells.

Virus infection

Retroviral vectors (pMXs or pSuper) were transfected into plat-E cells using PEI (PolyScience) transfection. After transfection for 48 h, the viral supernatants were collected and filtered prior to infecting MEFs with polybrene (Sigma) as described [55]. The infection would be repeated after 24 h.

iPSCs generation

Oct4, Sox2, Klf4, c-Myc and other plasmids were transfected to plat-E cells using PEI (Polyscience). OG2-MEFs were infected and then cultured in mESC medium (DMEM/High Glucose (HyClone) + 15% FBS (Gibco) + NEAA (Gibco) + GlutaMax (Gibco) + Sodium Pyruvate (Gibco) + β-Mercaptoethanol (Invitrogen) + lif) as described before [55, 56]. The iPSC colonies (GFP positive colonies) were picked out and identified. Chimeric mice and germline transmission mice were generated as described [55]. VPA was purchased from Sigma.

ITRAQ

Total proteins (100 μg) from each sample were denatured, cysteine blocked, and digested with trypsin as described in the standard protocol of iTRAQ (AB SCIEX, USA). Phospho-peptides were enriched by TiO2 beads (5020-75000 shimadzu), and separated with HPLC system (Easy nLC1000). Q-Exactive LC-MS (Thermo Finnigan) was used for protein identification and quantification.

Co-immunoprecipitation and western blot

Cells were lysed with RIPA (Beyotime Biotechnology, P0013B) and diluted in PBS. Total proteins and phosphor-proteins were analyzed by SDS-PAGE and then transferred to PVDF membrane (Millipore). After incubated with indicated antibodies, the membrane was exposed to X film. Anti-ACTIN (Sigma-Aldrich, A2228), anti-Mkk3 (Abcam, ab195037), anti-Mkk6 (Cell Signaling, 8550), anti-P38 (Cell Signaling, 8690), anti-p-P38 (Cell Signaling, 4511), anti-Gatad2b (Abcam, ab76924), anti-HA (Cell Signaling, 3724), anti-Flag (Sigma-Aldrich, F1804) and anti-p-Ser/Thr (Abcam, ab117253) were used.

To perform co-immunoprecipitation, Protein G beads (Invitrogen, 10004D) were incubated with Anti-Mkk6 and H3K9ac, H3K27ac, H4K16ac, H3 antibodies (Cell Signaling, 9649, 8173, 13534, 4499). Normal Rabbit IgG (Cell Signaling, 2729) was used as control. Western blot was used to test proteins. Protein signals were detected using SuperSignal West Pico kit (Thermo Scientific).

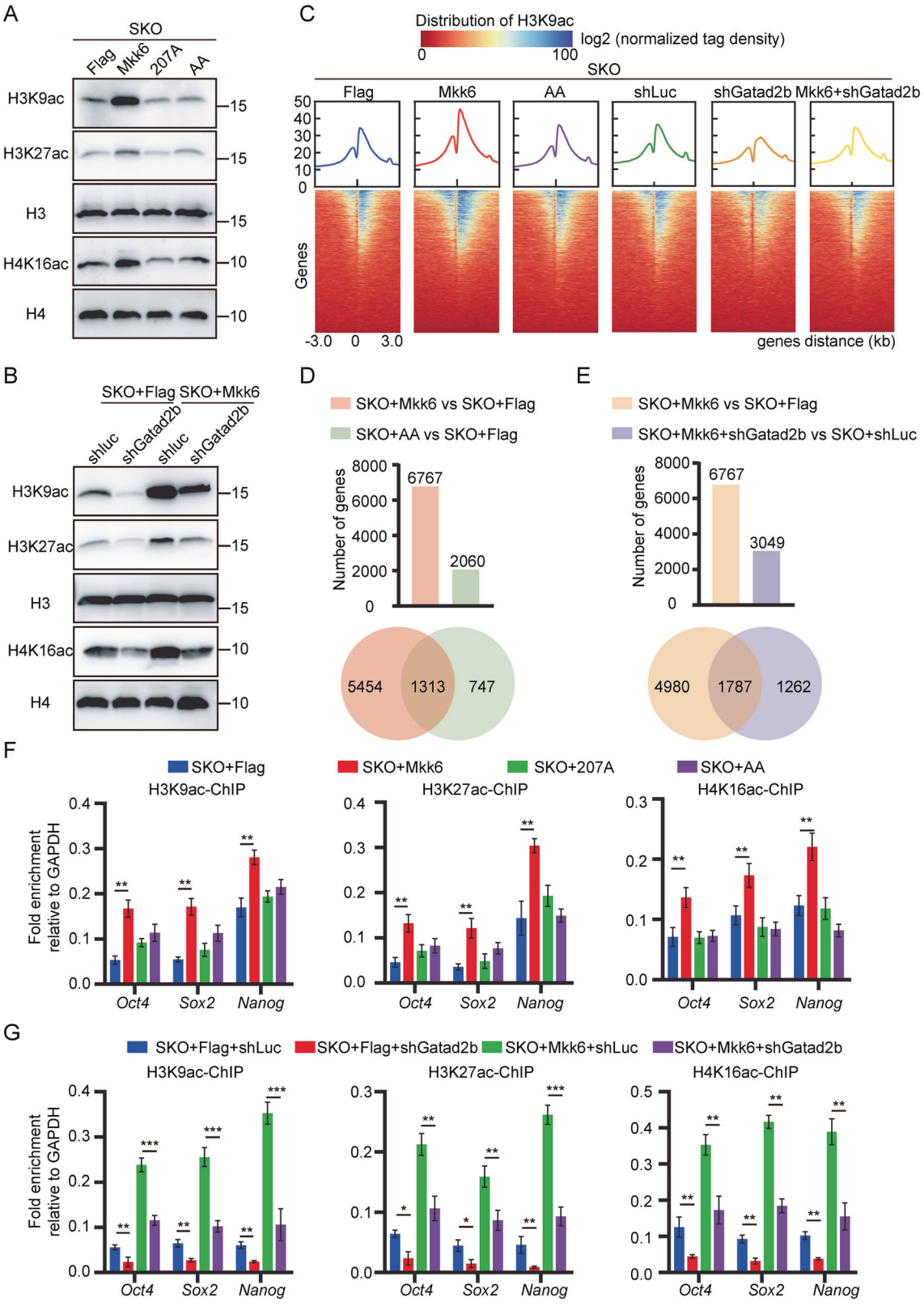

In vitro kinase assay

HEK293T cells were transfected with Mkk6-HA, AA-HA, Mkk3-HA, Gatad2b-3Flag and STAA-3Flag plasmids, respectively, and then the NP-40 buffer (Beyotime, P0013F) was used to lyse HEK293T cells. Gatad2b-3Flag and STAA-3Flag proteins were immunoprecipitated using anti-Flag beads (Sigma-Aldrich, A2220) from cells lysates and were kept on the beads which were washed by CK1 buffer (NEB, B6030S). Similarly, Mkk6-HA, Mkk3-HA and AA-HA proteins were immunoprecipitated using anti-HA beads (Sigma-Aldrich, A2095) from cell lysates. After three washes with CK1 buffer, the Mkk6-HA, Mkk3-HA and AA-HA proteins were eluted by

Fig. 5 Mkk6 increases histone acetylation through phosphorylation of Gatad2b. A Western blot analysis of H3K9ac, H3K27ac and H4K16ac in MEFs infected with SKO plus Flag, Mkk6 or its mutants. **B** Western blot analysis of H3K9ac, H3K27ac and H4K16ac in MEFs infected with SKO plus shLuc or shGatad2b in the presence or absence of Mkk6. **C** Tag density pileups of H3K9ac peaks at the indicated time points in MEFs transduced with SKO + Flag, SKO + Mkk6, SKO + AA, SKO + shLuc, SKO + shGatad2b and SKO + shGatad2b + Mkk6. **D** Number of genes with hyperacetylated promoter in MEFs infected with SKO + Mkk6 and SKO + AA, compared with SKO + Flag control. Venn diagram depicting overlap between them was shown. **E** Number of genes with hyperacetylated promoter in MEFs infected with SKO + Mkk6 and SKO + Mkk6 + shGatad2b, compared with SKO + Flag or SKO + shLuc control separately. Venn diagram depicting overlap between them was shown. **F** ChIP-qPCR analysis of H3K9ac, H3K27ac and H4K16ac in promoter regions of *Oct4*, *Sox2* and *Nanog* in MEFs infected with SKO plus Flag, Mkk6 or its mutants. Data were from three independent experiments and were shown as mean ± SD. $^{**}p \le 0.01$. **G** ChIP-qPCR analysis of H3K9ac, H3K27ac and H4K16ac in promoter regions of *Oct4*, *Sox2* and *Nanog* in MEFs infected with SKO plus shLuc or shGatad2b in the presence or absence of Mkk6. Data were from three independent experiments and were shown as mean ± SD. $^{*}p \le 0.05$; $^{**}p \le 0.01$; $^{***}p \le 0.001$.

CK1 buffer containing 0.5 mg/ml HA peptide (Beyotime, P9808) for 4 h at 4 °C. The elution was incubated with Gatad2b-3Flag or STAA-3Flag binding anti-Flag beads, then 6 mM ATP (Sigma-Aldrich, A2383) and phosphatase inhibitor cocktails (100×, Bimake, B15002) were added. The reaction was at 30 °C for 2 h and samples were further analyzed by western bolt.

Identification of Gatad2b Ser487 and T490 phosphorylation

Gatad2b-3Flag and Mkk3/6-HA were incubated in the presence of ATP in vitro. Then Gatad2b was resolved by SDS-PAGE, and the Gatad2b band was subjected to digestion using trypsin (ThermoFisher, 90057). Tryptic peptides were purified via MCX columns. Purified peptides were dried by speed vacuum and then resuspended in solvent (98:2:0.01, water: acetonitrile: formic acid) and analyzed by an Orbitrap XL mass spectrometer (ThermoFisher Scientific). Tandem MS data for the phosphorylated Gatad2b peptide was acquired using the ion trap mass analyzer in the ion trap (CID) mode. Peptide spectra were analyzed by MS/MS using Sequest (ThermoFisher Scientific, Inc., version 27) and the PEAKS software (Bioinformatics Solution Inc.).

RNA-seq and data analysis

Total RNA was isolated with TRIzol (Invitrogen). Libraries were prepared using the VAHTS mRNA-seq v2 Library Prep Kit for Illumina (NR601-01/02, Vazyme) following the manufacturer's instruction. Sequencing was performed using a MiSeq instrument at Annoroad Gene Technology (Beijing, China). Data were analyzed with RSEM (v.1.2.22) software and differentially expressed genes were obtained using DESeq2 (v.1.10.1). The P values represent the modified Fisher's exact corrected Expression Analysis Systematic Explorer (EASE) score.

ChIP-qPCR

ChIP assay was performed on day 8 during SKO reprogramming as described [18, 57]. Cells were incubated with 1% formaldehyde for crosslink. Then, the cells were harvested in PBS and lysed by lysis buffer and sonicated. Sheared chromatin was diluted with ChIP IP buffer. After antibodies coupled to Dynabeads with protein A and G (Invitrogen), the diluted chromatin was incubated with antibodies overnight at 4 °C. After immunoprecipitation, beads were washed with low-salt wash buffer, high-salt wash buffer, LiCl wash buffer and TE buffer. DNA was extracted with Chelex 100 and used for analysis. All the buffers were prepared as described [18]. ChIP-grade anti-Klf4, anti-Sox2, anti-Oct4 and control IgG were purchased from Millipore. H3K9, H3K27 and H4K16 acetylation antibodies and control IgG were purchased from Cell Signaling. Primers for *GAPDH* were: forward (5′-CCTTCATTGACCTCAACTACA-3′) and reverse (5′-TAGACTCCACGACATACTCA-3′) [10]. Primers for *Oct4* were: forward (5′-ATACTTGAACTGTGGTGGAG-3′) and reverse (5′-GCTATCATGCACCTTTGTTAT-3′). Primers for *Nanog* were: forward (5′-CAGGTGGGAAGTATCTATGG-3′) and reverse (5′-ACGGCTATTCTATTCAGTGG-3′). Primers for *Sox2* were: forward (5′-TTTATTCAGTTCCCAGTCCAA-3′) and reverse (5′-TTATTCCTATGTGTGAGCAAGA-3′). Primers for *Lefty* were: forward (5′-GTCCAGACAGGCTTTTGTGT-3′) and reverse (5′-AGTCTGCGGAGGAATGGTA-3′). Primers for *Chd1* were: forward (5′-CCATGTTAAAATGTCATTTA-3′) and reverse (5′-TGGAGTTACAAAGGACTTTA-3′). Primers for negative control (NC) were: forward (5′-AGCATGTGTTCTTCTTACCA-3′) and reverse (5′-GTTAGTTCATATTATTGTTCCACCTATA-3′).

ChIP-seq and data analysis

ChIP-seq was performed as previously described [58]. SimpleChIP Enzymatic Chromatin IP Kit (Magnetic Beads) (Cell Signalling Technology, 9003 S) was used to purify ChIP DNA and then the DNA was used for library construction and sequenced on a HiSeq 2000 instrument by Annoroad Gene Technology (Beijing, China). The antibodies for immunoprecipitation were acetyl-histone H3 (Lys9) (Cell Signalling Technology, no. 8173, 1:50).

The sequencing reads were mapped to the mouse reference sequence for the mouse genome (mm10) using Bowtie2 (v.2.2.5) with default parameters. Peaks were called using SICER (v.1.1.2) with 'W200 G200' parameters for H3K9ac modification on histone ChIP-seq data. Tracks of signal were computed using MACS2 bdgcmp module.pl module in HOMER (v.4.10.3) with the parameters '-len 8,10,12 -size 200'. The signal BigWig files were visualized using computeMatrix, plotHeatmap and plotProfile modules in DeepTools (v.2.4.2). Identification of nearby genes from the peaks obtained from MACS and SICER using ChIPpeakAnno (v.3.16.1). The BigWig tracks were visualized in the IGV browser (v.2.4.16).

ATAC-seq and data analysis

ATAC-seq was performed as previously described [26, 58]. Around 100,000 living cells were collected for each sample and the library construction and sequencing were carried out by Annoroad Gene Technology (Beijing, China). The ATAC library was sequenced on a NextSeq 500 using a NextSeq 500 High Output Kit v2 (150 cycles; FC-404-2002, Illumina).

The sequencing reads were filtered using Trimmomatic (v.0.35) and Cutadapt (v.1.13) and mapped to mouse reference sequence for mm10 using Bowtie2 (2.2.5) with parameters "-X2000 –local". Mapped reads were then sorted and deduplicated using Samtools (1.3.1) with parameters "-F 1804 -f 2 -q 30", and Picard tools MarkDuplicates (1.90). We performed peak calling using the MACS2 (2.1.0) callpeak module with parameters "-p 0.01 –nomodel-extsize 150 -B –SPMR –keep-dup all –call-summits" on pooled replicates, and then, only peaks with q value $<1 \times 10^{-5}$ were kept. Tracks of signal were computed using MACS2 bdgcmp module with parameter "-m ppois". Known and de novo motif analysis were conducted using findMotifsGenome.pl module in HOMER (4.10.3) with parameters "-len 8,10,12 -size 200". The signal BigWig files were visualized using computeMatrix, plotHeatmap, plotProfile, multiBigwigSummary, plotCorrelation, and plotPCA module in DeepTools (2.4.2). Signal density was computed using computeMatrix and Bedtools (2.25.0). ChIPpeakAnno (3.16.1) was used for identifying nearby genes from the peaks obtained from MACS. Differential binding genes were computed according to signal density using DESeq2 (1.22.2).

FRAP

MEFs infected with virus coding GFP-Histone1.4 and mCherry-HP1α were cultured in 35 mm dishes with glass bottom (WPI), and then infected with viruses coding the genes we tested. FRAP tests were taken 3 days post infection of the test genes with 100% power of 488 nm laser for bleaching, and micrographs were taken at 1 fps with Zeiss LSM 710 confocal microscopy with 512×512 resolution using a 100× oil objective. Bleach was confined to a series of oval areas of 25×25 pixels. FRAP curves were measured by ImageJ after stack-regulation and analyzed by Graphpad [59].

Nuclease accessibility assay

Nuclease accessibility assay was performed with EpiQ chromatin analysis kit (Bio-Rad). MEFs were infected with Flag, SKO, SKO plus Mkk6, 207 A or AA mutant. MEFs at each condition were divided into two groups: one was digested with the EpiQ nuclease, while the other not. The genomic DNA was purified and subjected to qPCR. The primers were designed from five different regions of *Oct4* promoter. Nuclease accessibility index was calculated after normalization to an internal control. Primers for P1 were: forward (5′-CTCTCGTCCTAGCCCTTCCT-3′) and reverse (5′-CCTCCACTCTGTCATGCTCA-3′). Primers for P2 were: forward (5′-CTGACCCTAGCCAACAGCTC-3′) and reverse (5′-TGCTCCTACACCATGCTCTG-3′). Primers for P3 were: forward (5′-CTTAGTGTCTTTCCGCCAGC-3′) and reverse (5′-TCCCCTCACACAAGACTTCC-3′). Primers for P4 were: forward (5′-GCACTTCTCTGG

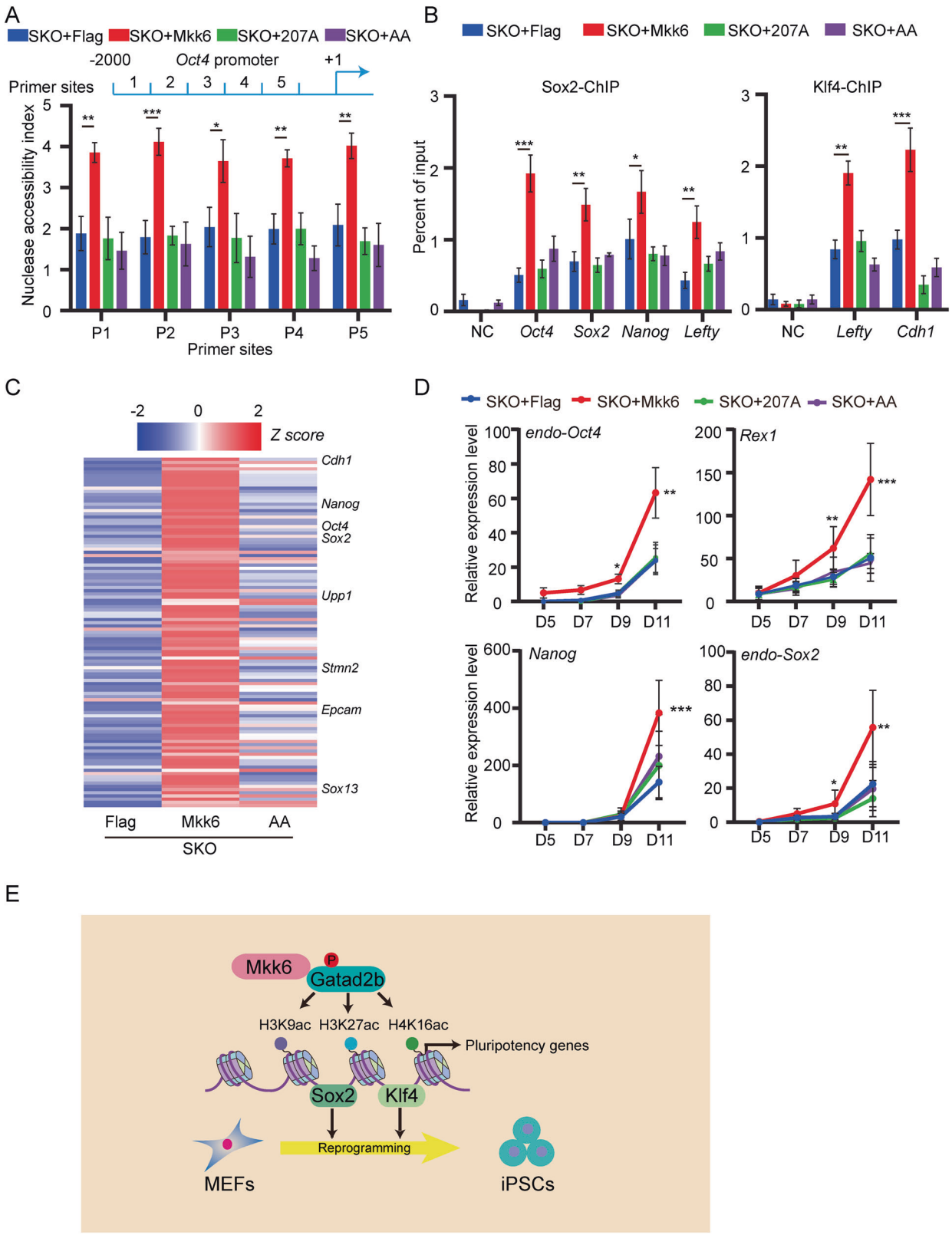

GGTCTCTG-3′) and reverse (5′-TGAACCCAGTATTTCAGCCC-3′). Primers for P5 were: forward (5′-CTGTAAGGACAGGCCGAGAG-3′) and reverse (5′-CAGG AGGCCTTCATTTTCAA-3′). Primers for *GAPDH* were: forward (5′-TGCGACTT CAACAGCAACTC-3′) and reverse (5′-CTTGCTCAGTGTCCTTGCTG-3′). Primers for *HBB* were: forward (5′-GAGTGGCACAGCATCCAGGGAGAAA-3′) and reverse (5-′CCACAGGCCAGAGACAGCAGCCTTC-3′).

Realtime PCR

Cells were cultured on 6 well dishes. Total RNA was isolated with TRIzol (invitrogen). RNA (5 μg) was used for reverse transcription with RNAce reagent (Toyobo). PCR reaction was performed with QPCR kits (Takara). Primers for *Mkk3* were: forward (5′- GCCTCAGACCAAAGGAAAATCC-3′) and reverse (5′- GGTGTGGGGTTGGACACAG-3′). Primers for *Mkk6* were: forward

Fig. 6 Mkk6 facilitates the binding ability of Sox2 and Klf4 and promotes the expression of pluripotency genes. A The chromatin compaction of different regions of the *Oct4* promoter was detected by nuclease accessibility assay. Genomic DNA was purified from MEFs infected with SKO plus Flag, Mkk6 or its mutants. Data were from three independent experiments and were shown as mean ± SD. *$p \le 0.05$; **$p \le 0.01$; ***$p \le 0.001$. **B** ChIP-qPCR analysis of the binding of Sox2 and Klf4 to their respective targets in MEFs infected with SKO plus Flag, Mkk6 or its mutants. Data were from three independent experiments and were shown as mean ± SD. *$p \le 0.05$; **$p \le 0.01$; ***$p \le 0.001$. **C** Heatmap of pluripotency genes according to RNA-seq in MEFs infected with SKO + Flag, SKO + Mkk6 and SKO + AA. **D** qPCR analysis of endogenous *Oct4*, *Rex1*, *Nanog* and *Sox2* expression levels during reprogramming with SKO plus Flag, Mkk6 or its mutants. Data were from three independent experiments and were shown as mean ± SD. *$p \le 0.05$; **$p \le 0.01$; ***$p \le 0.001$. **E** Scheme of Mkk6 loosening heterochromatin and enhancing reprogramming.

(5′- GCAAACCATACATGGCTCCT-3′) and reverse (5′- GCGTTCCCCAAGAATCATAA-3′). Primers for *Gatad2b* were: forward (5′- GGAAATTGAACAGCGATTACAGC-3′) and reverse (5′- GAAAGCATGGATCGGGCAGAT-3′). Primers for endo *Oct4* were: forward (5′-TAGGTGAGCCGTCTTTCCAC-3′) and reverse (5′-GCTTAGCCAGGTTCGAGGAT-3′). Primers for endo *Sox2* were: forward (5′-AGGGCTGGGAGAAAGAAGAG-3′) and reverse (5′-CCGCGATTGTTGTGATTAGT-3′). Primers for *Nanog* were: forward (5′-CTCAAGTCCTGAGGCTGACA-3′) and reverse (5′-TGAAACCTGTCCTTGAGTGC-3′). Primers for *Rex1* were: forward (5′-CCCTCGACAGACTGACCCTAA-3′) and reverse (5′-TCGG GGCTAATCTCACTTTCAT-3′). Primers for *Actin* were: forward (5′-TGCTAGGAGCCAGAGCAGTA-3′) and reverse (5′-AGTGTGACGTTGACATCCGT-3′).

Immunofluorescence

MEFs were infected with virus coding the genes of interest and then stained with antibody for HP1α (Cell Signaling, 2616) ($n \ge 8$). A Zeiss LSM 710 confocal microscopy was used for detection. The area of HP1α positive foci or DAPI foci was measured by Image-J using particles analysis.

Salt extraction assay

Cells were lysed in buffer A (0.32 M sucrose, 15 mM HEPES (pH 7.9), 60 mM KCl, 2 mM EDTA, 0.5 mM EGTA, 0.5% BSA, and 0.5 mM DTT), and centrifuged (15 min, 3000 *g*). Pelleted nuclei were resuspended in buffer B (15 mM HEPES (pH 7.9), 60 mM KCl, 15 mM NaCl, 0,34 mM sucrose, 10% glycerol), incubated with different NaCl concentrations (200–1000 mM) at 4 °C for 30 min, and centrifuged (15 min, 3000 *g*). The pellet remaining after salt treatment was extracted with 0.2 M H2SO4. Acid-soluble material was precipitated with 33% TCA (Fisher Scientific) and analyzed by western blot using anti-H3 antibody (Cell Signaling, 4499).

Statistical analysis

ATAC-seq, ChIP-seq and RNA-seq were performed twice and analyzed by one-way ANOVA with Dunnett's test or two-way ANOVA with Sidak correction. FRAP was performed three times and the data are expressed as mean ± SEM using two-tailed Student's *t* test. Other experiments were performed three times and are expressed as mean ± SD using two-tailed Student's *t* test. $P \le 0.05$ was considered statistically significant.

DATA AVAILABILITY

The Sequencing data reported in this paper has been deposited in the Genome Sequence Archive at the Beijing Institute of Genomics (BIG) Data Center, BIG, Chinese Academy of Sciences. The accession numbers for the ATAC-seq, ChIP-seq and RNA-seq data in this study are CRA005167, CRA005151 and CRA005159, which are publicly accessible at https://bigd.big.ac.cn/gsa.

REFERENCES

1. Takahashi K, Yamanaka S. Induction of pluripotent stem cells from mouse embryonic and adult fibroblast cultures by defined factors. Cell. 2006;126:663–76.
2. Huangfu DW, Maehr R, Guo WJ, Eijkelenboom A, Snitow M, Chen AE, et al. Induction of pluripotent stem cells by defined factors is greatly improved by small-molecule compounds. Nat Biotechnol. 2008;26:795–7.
3. Liang G, Taranova O, Xia K, Zhang Y. Butyrate promotes induced pluripotent stem cell generation. J Biol Chem. 2010;285:25516–21.
4. Mattout A, Biran A, Meshorer E. Global epigenetic changes during somatic cell reprogramming to iPS cells. J Mol Cell Biol. 2011;3:341–50.
5. Ang YS, Tsai SY, Lee DF, Monk J, Su J, Ratnakumar K, et al. Wdr5 mediates self-renewal and reprogramming via the embryonic stem cell core transcriptional network. Cell. 2011;145:183–97.
6. Mansour AA, Gafni O, Weinberger L, Zviran A, Ayyash M, Rais Y, et al. The H3K27 demethylase Utx regulates somatic and germ cell epigenetic reprogramming. Nature. 2012;488:409–13.
7. Zhao W, Li Q, Ayers S, Gu Y, Shi Z, Zhu Q, et al. Jmjd3 Inhibits Reprogramming by Upregulating Expression of INK4a/Arf and Targeting PHF20 for Ubiquitination. Cell. 2013;152:1037–50.
8. Wang T, Chen K, Zeng X, Yang J, Wu Y, Shi X, et al. The histone demethylases Jhdm1a/1b enhance somatic cell reprogramming in a vitamin-C-dependent manner. Cell Stem Cell. 2011;9:575–87.
9. Liang G, He J, Zhang Y. Kdm2b promotes induced pluripotent stem cell generation by facilitating gene activation early in reprogramming. Nat Cell Biol. 2012;14:457–66.
10. Chen J, Liu H, Liu J, Qi J, Wei B, Yang J, et al. H3K9 methylation is a barrier during somatic cell reprogramming into iPSCs. Nat Genet. 2013;45:34–42.
11. Apostolou E, Hochedlinger K. Chromatin dynamics during cellular reprogramming. Nature. 2013;502:462–71.
12. Singhal N, Graumann J, Wu G, Arauzo-Bravo MJ, Han DW, Greber B, et al. Chromatin-Remodeling Components of the BAF Complex Facilitate Reprogramming. Cell. 2010;141:943–55.
13. Gaspar-Maia A, Alajem A, Polesso F, Sridharan R, Mason MJ, Heidersbach A, et al. Chd1 regulates open chromatin and pluripotency of embryonic stem cells. Nature. 2009;460:863–8.
14. Wang L, Du Y, Ward JM, Shimbo T, Lackford B, Zheng X, et al. INO80 facilitates pluripotency gene activation in embryonic stem cell self-renewal, reprogramming, and blastocyst development. Cell Stem Cell. 2014;14:575–91.
15. Luo M, Ling T, Xie W, Sun H, Zhou Y, Zhu Q, et al. NuRD blocks reprogramming of mouse somatic cells into pluripotent stem cells. Stem Cells. 2013;31:1278–86.
16. Rais Y, Zviran A, Geula S, Gafni O, Chomsky E, Viukov S, et al. Deterministic direct reprogramming of somatic cells to pluripotency. Nature. 2013;502:65–70.
17. dos Santos RL, Tosti L, Radzisheuskaya A, Caballero IM, Kaji K, Hendrich B, et al. MBD3/NuRD facilitates induction of pluripotency in a context-dependent manner. Cell Stem Cell. 2014;15:102–10.
18. Chen K, Long Q, Wang T, Zhao D, Zhou Y, Qi J, et al. Gadd45a is a heterochromatin relaxer that enhances iPS cell generation. EMBO Rep. 2016;17:1641–56.
19. Wang B, Wu L, Li D, Liu Y, Guo J, Li C, et al. Induction of Pluripotent Stem Cells from Mouse Embryonic Fibroblasts by Jdp2-Jhdm1b-Mkk6-Glis1-Nanog-Essrb-Sall4. Cell Rep. 2019;27:3473–85 e3475.
20. Kim SH, Kim MO, Cho YY, Yao K, Kim DJ, Jeong CH, et al. ERK1 phosphorylates Nanog to regulate protein stability and stem cell self-renewal. Stem Cell Res. 2014;13:1–11.
21. Simone C, Forcales SV, Hill DA, Imbalzano AN, Latella L, Puri PL. p38 pathway targets SWI-SNF chromatin-remodeling complex to muscle-specific loci. Nat Genet. 2004;36:738–43.
22. Cargnello M, Roux PP. Activation and Function of the MAPKs and Their Substrates, the MAPK-Activated Protein Kinases. Microbiol Mol Biol R. 2011;75:50–83.
23. Long Q, Qi J, Li W, Zhou Y, Chen K, Wu H, et al. Protocol for detecting chromatin dynamics and screening chromatin relaxer by FRAP assay. STAR Protoc. 2021;2:100706.
24. Meshorer E, Yellajoshula D, George E, Scambler PJ, Brown DT, Misteli T. Hyperdynamic plasticity of chromatin proteins in pluripotent embryonic stem cells. Dev Cell. 2006;10:105–16.
25. Min X, Akella R, He H, Humphreys JM, Tsutakawa SE, Lee SJ, et al. The structure of the MAP2K MEK6 reveals an autoinhibitory dimer. Structure. 2009;17:96–104.
26. Chen K, Long Q, Xing G, Wang T, Wu Y, Li L, et al. Heterochromatin loosening by the Oct4 linker region facilitates Klf4 binding and iPSC reprogramming. EMBO J. 2020;39:e99165.
27. Moriguchi T, Kuroyanagi N, Yamaguchi K, Gotoh Y, Irie K, Kano T, et al. A novel kinase cascade mediated by mitogen-activated protein kinase kinase 6 and MKK3. J Biol Chem. 1996;271:13675–9.
28. Stein B, Brady H, Yang MX, Young DB, Barbosa MS. Cloning and characterization of MEK6, a novel member of the mitogen-activated protein kinase kinase cascade. J Biol Chem. 1996;271:11427–33.

29. Remy G, Risco AM, Inesta-Vaquera FA, Gonzalez-Teran B, Sabio G, Davis RJ, et al. Differential activation of p38MAPK isoforms by MKK6 and MKK3. Cell Signal. 2010;22:660–7.
30. Li Z, Rana TM. A kinase inhibitor screen identifies small-molecule enhancers of reprogramming and iPS cell generation. Nat Commun. 2012;3:1085.
31. Xu X, Wang Q, Long Y, Zhang R, Wei X, Xing M, et al. Stress-mediated p38 activation promotes somatic cell reprogramming. Cell Res. 2013;23:131–41.
32. Beausoleil SA, Villen J, Gerber SA, Rush J, Gygi SP. A probability-based approach for high-throughput protein phosphorylation analysis and site localization. Nat Biotechnol. 2006;24:1285–92.
33. Larsen MR, Thingholm TE, Jensen ON, Roepstorff P, Jorgensen TJ. Highly selective enrichment of phosphorylated peptides from peptide mixtures using titanium dioxide microcolumns. Mol Cell Proteom. 2005;4:873–86.
34. Unwin RD, Griffiths JR, Whetton AD. Simultaneous analysis of relative protein expression levels across multiple samples using iTRAQ isobaric tags with 2D nano LC-MS/MS. Nat Protoc. 2010;5:1574–82.
35. Yuan W, Wu T, Fu H, Dai C, Wu H, Liu N, et al. Dense chromatin activates Polycomb repressive complex 2 to regulate H3 lysine 27 methylation. Science. 2012;337:971–5.
36. Pearson G, Robinson F, Beers Gibson T, Xu BE, Karandikar M, Berman K, et al. Mitogen-activated protein (MAP) kinase pathways: regulation and physiological functions. Endocr Rev. 2001;22:153–83.
37. Dhanasekaran N, Premkumar Reddy E. Signaling by dual specificity kinases. Oncogene. 1998;17:1447–55.
38. Kouzarides T. Chromatin modifications and their function. Cell. 2007;128:693–705.
39. Rossetto D, Avvakumov N, Cote J. Histone phosphorylation: a chromatin modification involved in diverse nuclear events. Epigenetics. 2012;7:1098–108.
40. Klein AM, Zaganjor E, Cobb MH. Chromatin-tethered MAPKs. Curr Opin Cell Biol. 2013;25:272–7.
41. Bashir M, Parray AA, Baba RA, Bhat HF, Bhat SS, Mushtaq U, et al. beta-Amyloid-evoked apoptotic cell death is mediated through MKK6-p66shc pathway. Neuromolecular Med. 2014;16:137–49.
42. Feng Q, Cao R, Xia L, Erdjument-Bromage H, Tempst P, Zhang Y. Identification and functional characterization of the p66/p68 components of the MeCP1 complex. Mol Cell Biol. 2002;22:536–46.
43. Brackertz M, Gong Z, Leers J, Renkawitz R. p66alpha and p66beta of the Mi-2/NuRD complex mediate MBD2 and histone interaction. Nucleic Acids Res. 2006;34:397–406.
44. Brackertz M, Boeke J, Zhang R, Renkawitz R. Two highly related p66 proteins comprise a new family of potent transcriptional repressors interacting with MBD2 and MBD3. J Biol Chem. 2002;277:40958–66.
45. Torchy MP, Hamiche A, Klaholz BP. Structure and function insights into the NuRD chromatin remodeling complex. Cell Mol Life Sci. 2015;72:2491–507.
46. Mor N, Rais Y, Sheban D, Peles S, Aguilera-Castrejon A, Zviran A, et al. Neutralizing Gatad2a-Chd4-Mbd3/NuRD Complex Facilitates Deterministic Induction of Naive Pluripotency. Cell Stem Cell. 2018;23:412–25.
47. Fidalgo M, Faiola F, Pereira CF, Ding J, Saunders A, Gingold J, et al. Zfp281 mediates Nanog autorepression through recruitment of the NuRD complex and inhibits somatic cell reprogramming. Proc Natl Acad Sci USA. 2012;109:16202–7.
48. Wang S, Xia P, Ye B, Huang G, Liu J, Fan Z. Transient activation of autophagy via Sox2-mediated suppression of mTOR is an important early step in reprogramming to pluripotency. Cell Stem Cell. 2013;13:617–25.
49. Jaffer S, Goh P, Abbasian M, Nathwani AC. Mbd3 Promotes Reprogramming of Primary Human Fibroblasts. Int J Stem Cells. 2018;11:235–41.
50. Sakurai K, Talukdar I, Patil VS, Dang J, Li Z, Chang KY, et al. Kinome-wide functional analysis highlights the role of cytoskeletal remodeling in somatic cell reprogramming. Cell Stem Cell. 2014;14:523–34.
51. Vazquez-Martin A, Vellon L, Quiros PM, Cufi S, Ruiz de Galarreta E, Oliveras-Ferraros C, et al. Activation of AMP-activated protein kinase (AMPK) provides a metabolic barrier to reprogramming somatic cells into stem cells. Cell Cycle. 2012;11:974–89.
52. Yao K, Ki MO, Chen H, Cho YY, Kim SH, Yu DH, et al. JNK1 and 2 play a negative role in reprogramming to pluripotent stem cells by suppressing Klf4 activity. Stem Cell Res. 2014;12:139–52.
53. Tang Y, Luo Y, Jiang Z, Ma Y, Lin CJ, Kim C, et al. Jak/Stat3 signaling promotes somatic cell reprogramming by epigenetic regulation. Stem Cells. 2012;30:2645–56.
54. Wu Y, Chen K, Xing G, Li L, Ma B, Hu Z, et al. Phospholipid remodeling is critical for stem cell pluripotency by facilitating mesenchymal-to-epithelial transition. Sci Adv. 2019;5:eaax7525.
55. Esteban MA, Wang T, Qin B, Yang J, Qin D, Cai J, et al. Vitamin C enhances the generation of mouse and human induced pluripotent stem cells. Cell Stem Cell. 2010;6:71–79.
56. Chen J, Liu J, Chen Y, Yang J, Chen J, Liu H, et al. Rational optimization of reprogramming culture conditions for the generation of induced pluripotent stem cells with ultra-high efficiency and fast kinetics. Cell Res. 2011;21:884–94.
57. Nelson JD, Denisenko O, Sova P, Bomsztyk K. Fast chromatin immunoprecipitation assay. Nucleic Acids Res. 2006;34:e2.
58. Li L, Chen K, Wang T, Wu Y, Xing G, Chen M, et al. Glis1 facilitates induction of pluripotency via an epigenome-metabolome-epigenome signalling cascade. Nat Metab. 2020;2:882–92.
59. Thevenaz P, Ruttimann UE, Unser M. A pyramid approach to subpixel registration based on intensity. IEEE Trans Image Process. 1998;7:27–41.

ACKNOWLEDGEMENTS

We thank all the members in the labs of Prof DP and Prof XL. This work was financially supported by the National Key Research and Development Program of China (2018YFA0107100), the Strategic Priority Research Program of the Chinese Academy of Sciences (XDA16030505), the National Key Research and Development Program of China (2017YFA0106300, 2017YFA0102900, 2017YFA0504100, 2019YFA0904500), the National Natural Science Foundation projects of China (32025010, 31900614, 31970709, 81901275, 32070729, 32100619, 32170747, 31830060), the Key Research Program of Frontier Sciences, CAS (QYZDB-SSW-SMC001), and International Cooperation Program, CAS (154144KYSB20200006), Guangdong Province Science and Technology Program (2020B1212060052, 2018A030313825, 2018GZR110103002, 2020A1515011200, 2020A1515010919, 2020A1515011410, 2021A1515012513), Guangzhou Science and Technology Program (201807010067, 202002030277, 202102020827, 202102080066), Open Research Program of Key Laboratory of Regenerative Biology, CAS (KLRB201907, KLRB202014), and CAS Youth Innovation Promotion Association (to YW).

AUTHOR CONTRIBUTIONS

DP, XL, and KC supervised the project. DP, KC, and TW initiated wild-type and mutant Mkk6 effects on reprogramming efficiency. DP, XL, KC, GX, and DZ identified Mkk6's function depends on not P38 but Gatad2b, a novel target which acts downstream to elevate histone acetylation levels, loosen heterochromatin and facilitate binding of Sox2 and Klf4 to their targets and promotes pluripotency gene expression during reprogramming. XL, KC, DZ, GX, ZL, and HY designed and performed iPSCs generation, ITRAQ, co-IP, western blot, RNA-seq, ChIP-qPCR, ChIP-seq, ATAC-seq, in vitro kinase assay, nuclease accessibility assay and salt extraction assay. LH, ZH, YL, JLu, and SL participated in plasmids construction, iPSCs generation, and the dependence of Mkk6 function on P38. YW, LL, JZ, JW, and BW participated in cell culture and ChIP-qPCR. QL and YZ participated in FRAP and HP1α immunofluorescence. JLiu and JC participated in chimeric mice and germline transmission mice generation. DP, XL, KC, GX, ZL, and DZ wrote the paper. All authors contributed to the writing and editing of the paper and approved the final paper.

COMPETING INTERESTS

The authors declare no competing interests.

ETHICAL APPROVAL

All the cells were obtained with approval from the ethics committee of the Guangzhou Institutes of Biomedicine and Health, Chinese Academy of Sciences (GIBH). All the animals were handled according to approved Institutional Animal Care and Use Committee protocols of the GIBH.

ADDITIONAL INFORMATION

Supplementary information The online version contains supplementary material available at https://doi.org/10.1038/s41418-021-00902-z.

Correspondence and requests for materials should be addressed to Duanqing Pei, Xingguo Liu or Keshi Chen.

Reprints and permission information is available at http://www.nature.com/reprints

Publisher's note Springer Nature remains neutral with regard to jurisdictional claims in published maps and institutional affiliations.